•研究论文•

元胡止痛口服液化学成分表征及其治疗原发性痛经的作用机制初探

郑 韩[1,2], 付 璐[3], 钟余特[1], 李玮婕[1], 关建丽[4], 吴 丹[1,5*], 王 萍[1,2*], 许海玉[6]

(1. 中国中医科学院中药研究所, 道地药材品质保障与资源持续利用全国重点实验室, 北京 100700; 2. 中国中医科学院研究生院, 江苏 苏州 215105; 3. 江苏恒瑞医药股份有限公司, 江苏 连云港 222000; 4. 河南福森药业有限公司, 河南 南阳 474450; 5. 中国中医科学院博士后流动站, 北京 100700; 6. 辽宁中医药大学, 辽宁 大连 116600)

摘要: 本研究系统表征了元胡止痛口服液 (Yuanhu Zhitong Oral Liquid, YZOL) 的化学成分并探究其治疗原发性痛经 (primary dysmenorrhea, PD) 的作用机制。基于UPLC-Q-TOF-MS/MS技术, 共初步鉴定出100个成分, 主要为异喹啉类生物碱、香豆素类等; 通过苯甲酸雌二醇联合缩宫素建立大鼠PD模型, 从行为学指标、痛经相关因子水平及组织病理学变化等方面评价YZOL的干预效果, 结果显示YZOL能够有效减少PD大鼠扭体次数 ($P < 0.05$), 延长扭体潜伏期 ($P < 0.05$), 中、高剂量组显著降低$PGF_{2\alpha}$/PGE_2水平 ($P < 0.05$), 低、中、高剂量组均可显著降低TXB_2/6-keto-$PGF_{1\alpha}$水平 ($P < 0.05$), 同时明显改善子宫组织损伤, 高剂量组改善效果最为显著。进一步对子宫组织进行转录组测序, 分析共筛选得到403个回调基因, 其中YZOL-H *vs* PD上调280个, 下调123个。KEGG富集结果表明其主要涉及TGF-β信号通路、Rap1信号通路、PI3K-Akt信号通路、卵巢类固醇生成、MAPK信号通路等, 进一步功能注释表明, 这些通路与神经信号传导、炎症反应、突触活动及激素合成密切相关, 其异常激活可引起疼痛敏化、炎症介质释放及子宫平滑肌过度收缩, 从而促进PD的发生发展。结合转录组与网络药理学分析结果, 从疼痛信号传导、炎症反应调控及子宫平滑肌收缩等关键病理环节中筛选出7个核心靶点, 并采用AutoDock Vina进行分子对接分析。结果显示, YZOL中的黄连碱、紫花前胡苷、补骨脂素醇等与上述靶点具有较强结合活性, 结合能优于或接近阳性化合物, 且部分成分具有较高口服生物利用度 (oral bioavailability, OB), 提示其可能为体内主要药效成分。最终通过生物信息学分析及批量分子对接, 预测潜在活性成分与关键作用靶标之间的相互作用, 建立YZOL治疗PD的“活性成分−关键靶标−生物效应”多维网络。综上, 元胡止痛口服液中的黄连碱、紫花前胡苷、补骨脂素醇、二氢白屈菜红碱、欧前胡素可能作用于IL1B、PRKCG、TRPV1、PTGER2等靶点, 通过调控疼痛信号传导、炎症反应及子宫平滑肌收缩等过程, 而发挥抗原发性痛经的镇痛作用。实验获得中国中医科学院中药研究所实验动物伦理委员会的批准 (批准号: 2021B020)。

关键词: 元胡止痛口服液; 原发性痛经; UPLC-Q-TOF-MS/MS; 转录组学; 分子对接

中图分类号: R966 **文献标识码**: A **文章编号**: 0513-4870(2026)07-2464-15

收稿日期: 2025-11-03; 修回日期: 2026-02-25.

基金项目: 国家自然科学基金青年科学基金项目 (C类82505238); 中国博士后科学基金第77批面上资助 (2025M773916); 中央级公益性科研院所基本科研业务费专项资金资助 (ZXKT25041); 国家重点研发计划 (2023YFC2308200, 2023YFC3502900); 中国中医科学院科技创新工程项目资助 (CI2024E003).

*通讯作者 Tel: 86-10-64032656, E-mail: pwang@icmm.ac.cn;
Tel: 19800358761, E-mail: wudan111106@163.com

DOI: 10.16438/j.0513-4870.2025-1286

Preliminary exploration of the chemical characterization and mechanism of Yuanhu Zhitong Oral Liquid in the treatment of primary dysmenorrhea

ZHENG Han[1,2], FU Lu[3], ZHONG Yu-te[1], LI Wei-jie[1], GUAN Jian-li[4], WU Dan[1,5*], WANG Ping[1,2*], XU Hai-yu[6]

(*1. State Key Laboratory for Quality Ensurance and Sustainable Use of Dao-di Herbs, Institute of Chinese Materia Medica, China Academy of Chinese Medical Sciences, Beijing 100700, China;　2. Graduate School of China Academy of Chinese Medical Sciences, Suzhou 215105, China;　3. Jiangsu Hengrui Pharmaceuticals Co., Ltd., Lianyungang 222000, China;　4. Henan Fusen Pharmaceutical Co., Ltd., Nanyang 474450, China;　5. China Academy of Chinese Medical Sciences Post-doctoral Research Stations, Beijing 100700, China;　6. Liaoning University of Traditional Chinese Medicine, Dalian 116600, China*)

Abstract: This study systematically characterized the chemical composition of Yuanhu Zhitong Oral Liquid (YZOL) and elucidated its therapeutic mechanism in primary dysmenorrhea (PD). Using UPLC-Q-TOF-MS/MS, a total of 100 constituents were preliminarily identified in YZOL, predominantly isoquinoline alkaloids and coumarins. A rat model of PD was established by combined administration of estradiol benzoate and oxytocin, and the pharmacological effects of YZOL were comprehensively evaluated through behavioral assessment, quantification of dysmenorrhea-related mediators, and histopathological examination. The results demonstrated that YZOL significantly reduced writhing frequency and prolonged writhing latency in PD rats ($P < 0.05$). Specifically, medium- and high-dose YZOL markedly decreased the $PGF_{2\alpha}$/PGE_2 ratio ($P < 0.05$), while all dose groups significantly reduced the TXB_2/6-keto-$PGF_{1\alpha}$ ratio ($P < 0.05$). Consistently, YZOL treatment markedly ameliorated uterine histopathological damage, with the high-dose group exhibiting tissue morphology closest to normal. Transcriptomic profiling of uterine tissues identified 403 genes reversed by YZOL treatment, including 280 upregulated and 123 downregulated genes in the YZOL-H *versus* PD comparison. KEGG pathway enrichment analysis indicated that these reversed genes were primarily involved in the TGF-β, Rap1, PI3K-Akt, and MAPK signaling pathways, as well as ovarian steroidogenesis. Functional annotation further revealed that these pathways are closely associated with nociceptive signaling, inflammatory responses, synaptic activity, and hormone biosynthesis, and that their aberrant activation contributes to pain sensitization, inflammatory mediator release, and excessive uterine smooth muscle contraction during PD progression. Integrative analysis combining transcriptomics and network pharmacology identified seven core targets associated with key pathological processes, including pain transmission, inflammatory regulation, and uterine smooth muscle contraction. Molecular docking analysis using AutoDock Vina demonstrated that berberine, peucedanoside, bakuchiol alcohol, and other constituents exhibited strong binding affinities toward these targets, with binding energies comparable to or exceeding those of positive control compounds. In addition, several compounds showed favorable oral bioavailability, suggesting their potential contribution to the *in vivo* efficacy of YZOL. Based on bioinformatics analysis and batch molecular docking, a multidimensional "active component-key target-biological effect" network was constructed to systematically illustrate the therapeutic mechanism of YZOL against PD. Collectively, these findings indicate that YZOL exerts anti-dysmenorrheic effects through a multi-component, multi-target, and multi-pathway mode of action, in which key constituents including berberine, peucedanoside, bakuchiol alcohol, dihydrochelerythrine, and imperatorin may act on targets such as IL1B, PRKCG, TRPV1, and PTGER2 to coordinately modulate pain signaling, inflammatory responses, and uterine smooth muscle contraction. The experiment was approved by the Laboratory Animal Ethics Committee of the Institute of Chinese Materia Medica, China Academy of Chinese Medical Sciences (approval No. 2021B020).

Key words: Yuanhu Zhitong Oral Liquid; primary dysmenorrhea; UPLC-Q-TOF-MS/MS; transcriptome; molecular docking

痛经 (dysmenorrhea) 是指女性在月经期或前后出现下腹部痉挛性疼痛的临床综合征[1], 患病比例约为16.8%～90%[2]。根据病因及病理基础的不同, 痛经分为原发性痛经 (primary dysmenorrhea, PD) 和继发性痛经 (secondary dysmenorrhea, SD)。其中, PD又称为功能性痛经, 指在无生殖器官器质性病变情况下发生的痛经, 它是女性盆腔疼痛的最常见原因之一[3]。原发性痛经多起始于初潮或青春期早期, 主要表现为月经期子宫痉挛性疼痛, 疼痛多于经期首日达到高峰, 持续时间及程度因个体而异, 是青春期女性最常见的妇科疾病之一。关于其发病机制目前认为与前列腺素水平异常升高密切相关, 非甾体抗炎药 (NSAIDs) 通过抑制环氧化酶活性、减少前列腺素合成与释放, 从而成为临床治疗PD的主要药物[4]。然而, 长期或不当使用NSAIDs可能导致胃肠道不良反应、肝肾功能损伤及潜在的心血管风险[5]。中医学早在《金匮要略》中即有“经水不利, 少腹满痛”之记载, 认为痛经的病机主要与气滞血瘀、寒凝血瘀或气血亏虚等因素相关[6]。中医临床遵循“通则不痛”“荣则不痛”的治法治则, 常采用中药复方汤剂、中成药、针灸、耳穴压豆及穴位敷贴等多种方法综合干预, 以疏通经络、调和气血、缓解疼痛。随着中药制剂技术的革新, 治疗PD的给药形式日趋多样, 其中口服液剂型凭借其溶解度高、生物利用度好及起效迅速等优势, 在临床应用中占据重要地位[7]。临床实践中, 诸如复方益母草口服液[8]、血府逐淤口服液[9]及痛经口服液[10]等成熟制剂, 已广泛用于气滞血瘀、寒凝胞中等证型的辨证施治。这些制剂通过多机制协同干预, 不仅能有效缓解经期腹痛, 在改善乏力、情绪波动等伴随症状方面亦显示出良好效果, 且相较于固体制剂, 其剂量调节灵活, 尤其适合吞咽困难或依从性差的患者[11]。但亦存在贮藏稳定性差、口感接受度低、部分辅料不耐受及质量标准不一等问题[12]。

元胡止痛方具有理气、活血、止痛之功效, 临床上主要用于治疗气滞血瘀所致胃痛[13]、胁痛[14]、头痛[15]、痛经[16]及膝骨关节炎[17]等, 该方由醋制延胡索和白芷两味中药组成, 体现了“理气活血、止痛通络”的配伍原则。2025版《中华人民共和国药典》中收载了元胡止痛方6个剂型[18], 包括片剂、口服液、滴丸、胶囊、软胶囊和颗粒剂, 其中Zhang[19]采用元胡止痛片治疗PD, 可使患者痛经症状积分显著降低; 诸多研究报道元胡止痛胶囊、元胡止痛滴丸等多种剂型可显著减少痛经大鼠模型的扭体次数, 降低扭体率[20-22], 发挥良好的镇痛作用; 尽管口服液剂型在痛经治疗中展现出显著的临床价值, 但目前元胡止痛口服液 (Yuanhu Zhitong Oral Liquid, YZOL) 治疗PD仅停留在基础实验验证, 没有将成分和药效相关性进行联系。课题组[23-25]前期对元胡止痛方展开了大量研究, 且对元胡止痛口服液质量标准进行提升, 本研究在此基础上进一步对YZOL治疗PD的药理活性和作用机制展开研究, 通过建立大鼠PD模型, 结合转录组学筛选潜在靶点, 并对YZOL进行化学成分鉴定及分子对接验证活性成分−靶点作用, 旨在揭示YZOL多成分、多靶点协同作用特征, 阐明YZOL治疗PD的作用机制, 更深层次探讨其科学内涵。

材料与方法

实验动物 48只清洁级 (SPF) 雌性未孕未交配SD大鼠, 体重220 ± 20 g, 购自北京维通利华实验动物技术有限公司。实验动物饲养于中国中医科学院中药研究所动物房, 昼夜各12 h光照循环, 实验前适应性饲养5天, 自由摄食饮水, 实验室温度25 ± 1 ℃, 相对湿度60% ± 5%。所有研究均按照国际和国内动物实验的相关规定, 本研究获得中国中医科学院中药研究所实验动物伦理委员会的批准 [批准号: 2021B020, 许可证编号: SCXK (京) 2021-0006]。

药物与试剂 苯甲酸雌二醇注射液、缩宫素注射液购自宁波第二激素厂; 元胡止痛口服液 (批号220201) 由河南福森药业有限公司提供, 含生药材元胡479 mg·mL^{-1}、白芷240 mg·mL^{-1}; 布洛芬缓释胶囊购自中美天津史克制药有限公司; HE染色试剂盒购自北京索莱宝科技有限公司 (G1120); 前列腺素$F_{2\alpha}$ ($PGF_{2\alpha}$) 酶联免疫吸附测定试剂盒 (ELISA, 组织用)、前列腺素E_2 (PGE_2) ELISA试剂盒 (组织用)、6-酮−前列环素$F_{1\alpha}$ (6-keto-$PGF_{1\alpha}$) 试剂盒 (组织用)、血栓烷B_2 (TXB_2) ELISA试剂盒 (组织用) 均购自上海酶联生物技术有限公司; 延胡索乙素对照品 (批号110726-202020)、异欧前胡素对照品 (批号110827-202113) 购自中国食品药品检定研究院; 延胡索甲素对照品 (批号21111803) 购自北京百欧博伟有限公司; 欧前胡素对照品 (批号D07S10E97290)、白当归素对照品 (批号R29S9F71154) 购自上海源叶生物科技有限公司。

仪器 OLYMPUS显微镜 (日本Evident Corporation); BM450A型包埋机、BM450型组织包埋冷冻台 (派斯杰医疗); 石蜡切片机、Multiskan FC酶标仪 (美国Thermo Fisher Scientific); SYNAPT G2-Si质谱仪、ACQUITY超高效液相色谱仪、ACQUITY UPLC HSS T3色谱柱 (2.1 mm × 100 mm, 1.8 μm, 美国Waters Corporation)。

供试品溶液及混合对照品溶液制备 取YZOL 10 mL, 3 000 r·min^{-1}离心5 min后使用0.22 μm微孔滤

膜滤过, 即得供试品溶液。分别取延胡索乙素对照品、异欧前胡素对照品、延胡索甲素对照品、欧前胡素对照品、白当归素对照品适量, 用甲醇溶液超声溶解, 制成质量浓度为1 mg·mL^{-1}各对照品母液; 分取适量的各对照品溶液混合, 使用0.22 μm微孔滤膜过滤, 即得混合对照品溶液。

色谱条件　样品分析使用反相分离条件, 采用Waters公司UPLC超高效液相色谱, 梯度洗脱, 流动相为A (水, 0.1% 甲酸) 和B (乙腈, 0.1% 甲酸); 流速0.5 mL·min^{-1}; 柱温30 ℃, 进样量1 μL, 梯度洗脱 (0～2 min, 95% A→90% A; 2～7 min, 90% A→85% A; 7～20 min, 85% A→77% A; 20～23 min, 77% A→73% A; 23～27 min, 73% A→50% A; 27～30 min, 50% A→2% A; 30～33 min, 2% A; 33～33.2 min, 2% A→95% A)。

质谱条件　质谱条件采用电喷雾电离正离子(ESI+) 扫描模式, 数据使用MSE Continuum模式采集。脱溶剂气为氮气, 流速为900 L·h^{-1}, 温度为450 ℃, 离子源温度为100 ℃。扫描时间为0.2 s, 扫描范围为*m*/*z* 50～1 200 Da。碰撞气体为氩气, 碰撞能量为40～60 eV。由MassLynx V4.2软件控制液质系统、数据采集和分析数据。使用leucine enkephalin (*m*/*z* 556.277 1 ESI+) 作校正液。

化学成分分析　取“供试品溶液及混合对照品溶液制备”项下样品溶液, 按“质谱条件”项下色谱与质谱条件进样。采用由MassLynx V4.2软件分析各成分峰的分子离子和碎片离子信息, 结合UNIFI 1.8软件预测、化合物精确质量数、二级裂解碎片和相关文献, 对元胡止痛口服液的化学成分进行鉴定或推测。

PD模型构建、分组与给药　采用苯甲酸雌二醇联合缩宫素构建大鼠PD模型。将48只雌性SD大鼠随机分组, 每组8只, 分别为空白对照组 (control)、模型对照组 (model)、元胡止痛口服液低、中、高剂量组 (1.08 g·kg^{-1}, YZOL-L; 3.24 g·kg^{-1}, YZOL-M; 9.72 g·kg^{-1}, YZOL-H), 阳性对照组 (0.07 g·kg^{-1}, 布洛芬 ibuprofen)。空白对照组的大鼠皮下注射等量生理盐水, 其余各组大鼠均皮下注射苯甲酸雌二醇[26] (第1、10天注射剂量为2.5 mg·kg^{-1}·d^{-1}, 第2～9天注射剂量为1.25 mg·kg^{-1}·d^{-1})。自注射苯甲酸雌二醇第4天起, 于注射半小时后灌胃给药相应剂量的元胡止痛口服液或布洛芬, 空白对照组和模型对照组大鼠灌胃等量生理盐水, 每天1次, 连续7天。第10天, 注射苯甲酸雌二醇1 h后腹腔注射缩宫素10 U·kg^{-1}, 空白对照组腹腔注射等量生理盐水, 用于大鼠PD模型构建。

扭体次数和扭体潜伏期检测　造模第10天, 各组大鼠腹腔注射缩宫素后, 记录注射后0～30 min内大鼠的扭体次数及首次扭体出现时间, 即扭体潜伏期。

ELISA法检测子宫相关因子表达水平　收集各组大鼠子宫组织, 制成匀浆液, 于5 000 r·min^{-1}条件下离心10 min, 取上清液检测。采用ELISA法测各实验组大鼠子宫组织匀浆中$PGF_{2\alpha}$、PGE_2、TXB_2、6-keto-$PGF_{1\alpha}$水平, 按照试剂盒说明书严格进行测定。

H&E染色观察各实验组大鼠子宫病理学变化　切取新鲜的大鼠子宫组织1～2 cm, 放入10%福尔马林进行固定, 然后进行常规脱水、透明、浸蜡、包埋与切片、脱蜡、苏木素伊红染色等步骤, 显微镜下观察各组大鼠子宫的病理学变化, 并获取具有代表性的组织切片影像以供分析。

转录组学测序与分析　采用转录组学方法对各实验组大鼠子宫组织的差异基因进行检测。首先使用RNA提取试剂盒从子宫组织中提取总RNA, 检测RNA完整性, 并对总RNA进行浓度及纯度检测。参考mRNA-seq Lib Prep Kit (Abclonal公司) 说明书构建文库, 并进行生物信息学分析。去除原始fastq文件内不合格的reads得到clean reads。将获得的clean reads与已知的参考基因组比对, 根据基因比对到参考基因组的物理位置信息, 统计每个基因从起始到终止范围内覆盖的reads数。根据基因表达丰度、其在转录本上的位置、转录本长度及测序深度计算每个基因的FPKM值。筛选差异基因 (DEGs) 标准为|FC| > 1.3, P < 0.05, 同时任意一组FPKM > 1。对DEGs进行基于GO (gene ontology) 及KEGG (Kyoto encyclopedia of genes and genomes) 数据库的功能注释。

元胡止痛口服液功效组网络调控机制研究　基于转录组测序结果筛选得到的DEGs与预测的YZOL候选靶标进行整合分析, 去除重复及无交互关系的基因节点后, 通过STRING v11.0平台 (https://www.string-db.org/) 提取蛋白相互作用信息, 进而构建“YZOL候选靶标干预PD相关基因”互作网络; 通过Cytoscape 3.10.0软件对网络进行分析, 计算度值、介数中心性、接近中心性的网络拓扑特征值, 以中位数为卡值, 选择同时大于这3个指标中位数的靶标, 筛选出YZOL治疗PD的核心靶标。通过DAVID v6.8在线生物信息分析平台 (david.abcc.ncifcrf.gov/) 对其生物功能进行注释和富集分析 (显著性标准: P < 0.05 目 Benjamini 校正 P < 0.05), 以挖掘YZOL治疗PD的生物学功能。

活性成分与靶蛋白的分子对接与可视化分析　采用AutoDock Vina软件对YZOL筛选得到的关键化学成分与疾病相关靶点进行分子对接分析。靶点选自与PD生物学功能相关的7个核心基因。关键成分的三维结构文件 (.sdf) 来源于PubChem数据库 (https://

pubchem.ncbi.nlm.nih.gov/), 并经 OpenBabel 转换为 PDBQT 格式。靶蛋白的晶体结构自 RCSB PDB 数据库 (https://www.rcsb.org/) 获取, 导入前对其进行预处理, 包括去除水分子、添加氢原子及修复缺失残基等操作。随后使用 AutoDock Vina 进行分子对接计算, 获取各配体与受体的结合能 (binding affinity, kcal·mol^{-1}), 并筛选能量最低的构象作为最佳对接模型, 用以预测活性成分与靶点间的结合模式。选取结合能较低的复合物, 利用 PyMOL 和 Discovery Studio Visualizer 软件进行可视化展示, 分析氢键、疏水相互作用、π-π 堆积等结合形式及关键氨基酸残基的参与情况, 从而揭示活性成分与靶点的作用特征。

数据统计与处理 所有数据均采用 GraphPad Prism 8.0.2 统计软件进行统计分析, 实验结果以均数 ± 标准差 ($\bar{x} \pm s$) 表示, 正态分布资料采用单因素方差分析比较多组间差异, 偏态分布资料采用 Wilcoxon 秩和检验分析, $P < 0.05$ 表示差异有统计学意义。

结果

1 YZOL 的化学成分分析

采用 UPLC-Q-TOF-MS/MS 对 YZOL 进行化学成分分析, 共鉴定推测出化学成分 100 个, 主要成分包括香豆素类、生物碱类 (如原小檗碱类、阿朴芬类、异喹啉类、原阿片碱类等)、萜类化合物及有机酸类等。样品正离子色谱峰和对照品正离子色谱图见图 1, 化合物鉴定结果见表 1。

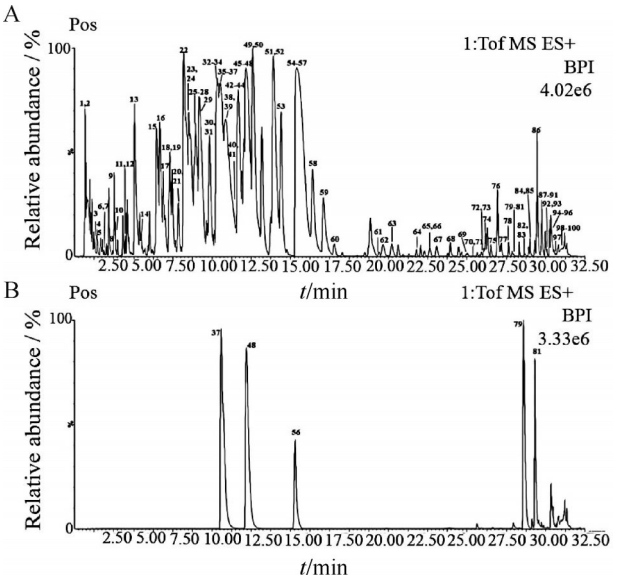


Figure 1 Base peak ion diagram of Yuanhu Zhitong Oral Liquid (YZOL) (A) and mixed standards (B) in positive ion mode

Table 1 Composition analysis of YZOL by UPLC-Q-TOF-MS/MS. YHS: Corydalis Rhizoma; BZ: Angelicae Dahuricae Radix

NO.	Observed RT/min	Adducts	Component name	Formular	Neutral mass (*m/z*)	Observed *m/z*	Mass error (ppm)	Fragments	Source	Category
1	0.69	+H	*N*-Methyl-tetrahydropalmatine	$C_{22}H_{28}NO_4$	370.201 83	371.209 8	1.9	311.169 6	YHS	Others
2	0.69	+H	*L*(+)-Arginine	$C_6H_{14}N_4O_2$	174.111 68	175.117 8	−6.7	112.073 9	BZ	Amino acids
3	1.07	+H	Adenosine	$C_{10}H_{13}N_5O_4$	267.096 75	268.103	−3.9	136.064 4, 119.039 3, 85.028 7	YHS	Others
4	1.2	+Na	*D*-Lactose	$C_{12}H_{22}O_{11}$	342.116 21	365.104 3	−3.2	325.113 1, 145.048 1	YHS	Saccharides
5	1.45	−e	*N*-Carbobenzoxy-*DL*-leucine	$C_{14}H_{19}NO_4$	265.131 41	265.129 6	−4.9	210.086 9	BZ	Others
6	1.61	+H	Desmodimine	$C_{12}H_{15}NO_4$	237.100 11	238.108 3	4	210.086 9	BZ	Pyrroles
7	1.95	+Na	Atractylon	$C_{15}H_{20}O$	216.151 42	239.142	5.8	202.093 1, 162.079 5, 135.031 7	BZ	Terpenoids
8	2.42	+Na	(8*E*)-1,8-Heptadecadiene-4, 6-diyne-3,10-diol	$C_{17}H_{24}O_2$	260.177 63	283.165	−6.4	175.116 7	BZ	Others
9	2.49	+H	Adenine	$C_5H_5N_5$	135.054 5	136.060 7	−7.6	119.035 4	BZ	Others
10	2.6	+Na	*D*-Phenylalanine	$C_9H_{11}NO_2$	165.078 98	188.069 3	5.8	91.055 5	YHS	Amino acid
11	3.23	+H	7-Hydroxycoumarin	$C_9H_6O_3$	162.031 69	163.037 7	−7.7	135.044 0	BZ	Coumarins
12	3.23	+Na	Isoscopolin	$C_{16}H_{18}O_9$	354.095 08	377.083 7	−1.6	298.108 7	BZ	Coumarins
13	3.81	+Na	Stearic acid/palmitic acid ethyl ester	$C_{18}H_{36}O_2$	284.271 53	307.258 8	−6.4	117.031 6	YHS	Fatty acids
14	4.22	+H	Taxilamine	$C_{20}H_{19}NO_6$	369.121 24	370.127 9	−1.8	308.091 2	YHS	Others
15	5.26	+H	Smyrindiol	$C_{14}H_{14}O_5$	262.084 12	263.090 7	−2.7	176.063 6	BZ	Coumarins
16	5.42	+H	Coreximine/scoulerine	$C_{19}H_{21}NO_4$	327.147 06	328.153 6	−2.2	178.087 1	YHS	Apophis
17	5.64	+H	*N*-Methyllaurotetanie/ norglaucine/ tetrahydrocolumbamine/ tetrahydrojatrorrhizine	$C_{20}H_{23}NO_4$	341.162 71	342.168 9	−3.2	178.087 1, 163.062 3	YHS	Apophis

Continued

NO.	Observed RT/min	Adducts	Component name	Formular	Neutral mass (*m/z*)	Observed *m/z*	Mass error (ppm)	Fragments	Source	Category
18	6.01	+H	8-Oxocoptisine	$C_{19}H_{13}NO_5$	335.079 37	336.085 9	−2.2	320.093 2, 292.098 3	YHS	Protoberberines
19	6.02	+H	Pulbocapnine	$C_{19}H_{19}NO_4$	325.131 41	326.137 6	−3.2	189.069 4	YHS	Apophis
20	6.66	+H	Noroxyhydrastinine	$C_{10}H_9NO_3$	191.058 24	192.064 2	−6.7	176.068 2, 148.073 6	YHS	Others
21	6.76	+H	Bicuculline	$C_{20}H_{17}NO_6$	367.105 59	368.112 5	−1	352.151 0, 321.095 3, 234.092 9, 148.073 6	YHS	Others
22	6.96	+H	Corydalmine	$C_{20}H_{23}NO_4$	341.162 71	342.169 6	−1.3	178.087 1, 163.062 3	YHS	Protoberberines
23	7.17	+H	Berberrubine	$C_{19}H_{15}NO_4$	321.100 11	322.106 3	−3.3	250.083 0, 134.060 0	YHS	Protoberberines
24	7.27	+H	Corybulbine/isocorybulbine	$C_{21}H_{25}NO_4$	355.178 36	356.187	3.9	192.101 7, 177.078 6	YHS	Protoberberines
25	7.48	+H	(+)-Dihydrooroselol/marmesin	$C_{14}H_{14}O_4$	246.089 21	247.095 3	−4.8	177.078 6, 91.052 1	BZ	Coumarins
26	7.49	+Na	Nodakenin	$C_{20}H_{24}O_9$	408.142 03	431.131 1	−0.3	342.169 2, 163.062 3	BZ	Coumarins
27	7.7	−e	Thaliporphine	$C_{20}H_{23}NO_4$	341.162 71	341.160 1	−6	192.101 7	YHS	Apophis
28	7.71	+H	Corybulbine/isocorybulbine	$C_{21}H_{25}NO_4$	355.178 36	356.185 6	0	192.101 7, 177.078 6	YHS	Protoberberines
29	7.94	+H	Protopine	$C_{20}H_{19}NO_5$	353.126 32	354.133 3	−0.9	336.121 2, 206.075 6	YHS	Proto-opioids
30	8.27	−e	Corydayanine	$C_{20}H_{20}NO_4$	338.139 23	338.137 8	−2.7	323.116 9, 308.091 2, 294.111 1, 279.089 5	YHS	Protoberberines
31	8.58	+H	Yuanhunine/norcoralydine	$C_{21}H_{25}NO_4$	355.178 36	356.184 8	−2.2	178.087 1	YHS	Protoberberines
32	9.01	−e	13-Methyl-dehydrocorydalmine	$C_{20}H_{20}NO_4$	338.139 23	338.137 4	−3.9	323.110 6, 322.108 0, 308.085 0, 294.111 1	YHS	Protoberberines
33	9.03	+H	Homochelidonine	$C_{21}H_{23}NO_5$	369.157 62	370.163 9	−2.7	165.068 7, 152.062 2	YHS	Isoquinolines
34	9.06	+H	*D*-Glaucine	$C_{21}H_{25}NO_4$	355.178 36	356.187 6	5.6	295.095 9, 279.101 3, 251.108 3	YHS	Apophis
35	9.21	−e	Stepharanine	$C_{19}H_{18}NO_4$	324.123 58	324.121 6	−4.3	176.068 2	YHS	Protoberberines
36	9.23	+H	Leonticine	$C_{20}H_{25}NO_3$	327.183 44	328.189 7	−3.1	283.120 4, 175.060 8	YHS	Others
37	9.34	+H	Tetrahydropalmatine	$C_{21}H_{25}NO_4$	355.178 36	356.187 6	5.6	310.108 7, 294.111 1, 192.101 7, 165.091 3	YHS	Protoberberines
38	9.55	−e	Coptisine	$C_{19}H_{14}NO_4$	320.092 28	320.091 4	−1.1	318.074 9, 292.092 3, 277.070 3, 262.085 8	YHS	Protoberberines
39	9.79	+H	2,3,9,10-Tetramethoxy-13-methyl-5,8,13,13a-tetrahydro-6hisoquino[3,2-a]isoquinoline	$C_{22}H_{27}NO_4$	369.194 01	370.200 2	−2.8	206.116 1, 176.063 6	YHS	Isoquinolines
40	10.16	+H	*DL*-Stylopine	$C_{19}H_{17}NO_4$	323.115 76	324.122 2	−2.5	262.085 8, 233.081 5	YHS	Protoberberines
41	10.17	+H	*N*-Methyl-canadine	$C_{21}H_{24}NO_4$	354.170 53	355.176 5	−3.7	262.085 8, 204.079 5	YHS	Others
42	10.41	+H	Tetrahydroberberine	$C_{20}H_{21}NO_4$	339.147 06	340.153 7	−1.9	176.068 2	YHS	Protoberberines

Continued

NO.	Observed RT/min	Adducts	Component name	Formular	Neutral mass (*m*/*z*)	Observed *m*/*z*	Mass error (ppm)	Fragments	Source	Category
43	10.42	−e	Columbamine	$C_{20}H_{20}NO_4$	338.139 23	338.137 4	−3.8	176.068 2, 161.045 9	YHS	Protoberberines
44	10.53	+H	Dehydroglaucine	$C_{21}H_{23}NO_4$	353.162 71	354.168 5	−4.2	149.060 4	YHS	Apophis
45	10.65	+H	*α*-Allocryptopine	$C_{21}H_{23}NO_5$	369.157 62	370.163 9	−2.7	352.151 0, 290.086 4	YHS	Proto-opioids
46	10.78	+H	(+)-Cavidine	$C_{21}H_{23}NO_4$	353.162 71	354.169 1	−2.5	190.087 2, 165.091 3	YHS	Protoberberines
47	10.79	+H	*O*-Methylbulbocapnine	$C_{20}H_{21}NO_4$	339.147 06	340.153 2	-3.4	190.087 2	YHS	Apophis
48	10.9	+H	Corydaline	$C_{22}H_{27}NO_4$	369.194 01	370.202 8	4.1	206.116 1, 165.091 3	YHS	Protoberberines
49	11.33	+Na	Isoboldine	$C_{19}H_{21}NO_4$	327.147 06	350.139	7.7	250.088 5, 176.068 2	YHS	Apophis
50	11.35	−e	13-Methylpalmatrubine/13-methyl-columbamine	$C_{21}H_{22}NO_4$	352.154 88	352.154 1	−0.8	337.128 7, 336.121 2, 322.105 3, 308.128 3, 294.111 1	YHS	Protoberberines
51	12.65	−e	Palmatine	$C_{21}H_{22}NO_4$	352.154 88	352.153 7	−1.9	337.128 7, 336.121 2, 322.105 3, 308.128 3, 294.111 1	YHS	Protoberberines
52	12.74	−e	Berberine	$C_{20}H_{18}NO_4$	336.123 58	336.122	−3	321.095 3, 320.093 2, 292.098 3, 278.079 0	YHS	Protoberberines
53	13.15	+H	Oxypeucedanin hydrate/heraclenol	$C_{16}H_{16}O_6$	304.094 69	305.101 2	−2.4	203.034 9, 175.037 5, 159.042 1, 147.043 2	BZ	Coumarins
54	14.11	−e	Dehydrocorydaline	$C_{22}H_{24}NO_4$	366.170 53	366.171 3	3.6	350.139 2, 322.105 3, 308.128 3	YHS	Protoberberines
55	14.15	+H	Anhydrobyankangelicin/apaensin/byakangelicol	$C_{17}H_{16}O_6$	316.094 69	317.100 7	−4	233.081 5, 175.037 5	BZ	Coumarins
56	14.15	+Na	Byakangelicin	$C_{17}H_{18}O_7$	334.105 25	357.093 3	−3.3	317.102 5, 231.027 9, 203.034 9	BZ	Coumarins
57	14.77	+H	Isopsoralen	$C_{11}H_6O_3$	186.031 69	187.037 9	−5.6	147.043 2, 129.101 9, 121.064 1	BZ	Coumarins
58	15.28	+H	Saulatine	$C_{22}H_{23}NO_6$	397.152 54	398.159 8	0	336.121 2, 321.101 6	YHS	Isoquinolines
59	15.85	+H	Oxoglaucine	$C_{20}H_{17}NO_5$	351.110 67	352.117 1	−2.3	306.074 2, 178.063 6	YHS	Apophis
60	16.55	+H	Xanthotoxin	$C_{12}H_8O_4$	216.042 26	217.048 3	−5.6	202.023 0, 161.059 3	BZ	Coumarins
61	19.4	+H	Angelol A/angelol H	$C_{16}H_{14}O_4$	376.152 2	377.158 8	−1.7	334.104 4, 320.093 2	BZ	Coumarins
62	19.66	+H	Bergapten	$C_{12}H_8O_4$	216.042 26	217.048 4	−5.2	202.023 0, 174.028 4	BZ	Coumarins
63	20.21	+H	pimpinellin	$C_{13}H_{10}O_5$	246.052 82	247.058 9	−4.7	232.034 8, 217.015 4	BZ	Coumarins
64	21.79	+H	Myrtenylacetate	$C_{12}H_{18}O_2$	194.130 68	195.136 6	−7	149.021 7, 105.069 5	BZ	Coumarins

Continued

NO.	Observed RT/min	Adducts	Component name	Formular	Neutral mass (*m*/*z*)	Observed *m*/*z*	Mass error (ppm)	Fragments	Source	Category
65	22.64	+H	Oxypeucedanin/prangenin/ isooxypeucedanin/ isoheraclenin/pabulenol	$C_{16}H_{14}O_5$	286.084 12	287.090 4	−3.4	203.034 9, 175.037 5, 159.046 5, 147.043 2	BZ	Coumarins
66	22.65	+H	Xanthotoxol	$C_{11}H_6O_4$	202.026 61	203.032 8	−5.1	175.037 5, 147.043 2	BZ	Coumarins
67	23.07	+Na	Byakangelicol/7*H*-Furo[3,2-*g*][1]benzopyran-7-one,9-methoxy-4-(3-methyl-2-oxobutoxy)	$C_{17}H_{16}O_6$	316.094 69	339.082 8	−3.3	231.027 9, 188.010 9	BZ	Coumarins
68	23.96	+Na	2-Undecanone	$C_{11}H_{22}O$	170.167 07	193.157 6	6.6	85.028 7	BZ	Others
69	25.02	+H	Pontevedrine	$C_{21}H_{19}NO_6$	381.121 24	382.127 8	−1.7	352.157 6, 149.021 7	YHS	Apophis
70	25.39	+K	Isodemethylfuropinarine/ demethylfuropinarine	$C_{17}H_{16}O_4$	284.104 86	323.067 9	−0.4	183.039 2, 178.082 4	BZ	Coumarins
71	25.44	+Na	Methyl 11,14-eicosadienoate	$C_{21}H_{38}O_2$	322.287 18	345.274 3	−6.2	292.098 3, 250.177 6	BZ	Others
72	25.78	+H	Oxypeucedanin/prangenin/ isooxypeucedanin/ isoheraclenin/pabulenol	$C_{16}H_{14}O_5$	286.084 12	287.090 5	−3	203.024 9, 175.037 5, 159.042 1, 147.047 4	BZ	Coumarins
73	25.89	+H	Anhydrobyankangelicin/ apaensin/byakangelicol	$C_{17}H_{16}O_6$	316.094 69	317.101 2	−2.3	233.081 5, 218.022 6, 203.034 9, 175.037 5	BZ	Coumarins
74	26.18	+H	Luguine	$C_{19}H_{13}NO_5$	335.079 37	336.085 1	−4.6	308.091 2	YHS	Others
75	26.45	+H	Osthenol	$C_{14}H_{14}O_3$	230.094 29	231.100 4	−5.1	147.043 2, 91.055 5	BZ	Coumarins
76	26.93	+H	9-(3,3-Dimethyl-oxiranylmethyl)-furo[3,2-*g*]chromen-7-one	$C_{16}H_{14}O_4$	270.089 21	271.095 3	−4.2	241.048 2, 227.069 7, 229.047 2	BZ	Others
77	27.16	+Na	Scoparone	$C_{11}H_{10}O_4$	206.057 91	229.048 6	6.6	145.065 1, 103.051 5	BZ	Coumarins
78	27.57	+Na	7-Hydroxy-6-(3-methyl-2-butenoxy)-coumarin	$C_{14}H_{14}O_4$	246.089 21	269.080 4	7.1	204.084 5	BZ	Coumarins
79	27.95	+H	Imperatorin	$C_{16}H_{14}O_4$	270.089 21	271.095 4	−3.9	203.034 9, 159.042 1, 147.043 2	BZ	Coumarins
80	27.95	+Na	Scopoletin/isoscopletin	$C_{10}H_8O_4$	192.042 26	215.033	7.1	131.048 9	BZ	Coumarins
81	28.12	+H	Isoimperatorin	$C_{16}H_{14}O_4$	270.089 21	271.095 6	−3.3	203.034 9, 159.042 1, 147.043 2	BZ	Coumarins
82	28.64	+Na	A bifuranocoumarin formed by a byakangelicin and neobyakangelicol	$C_{34}H_{34}O_{13}$	650.199 94	673.190 8	2.4	437.193 6, 231.027 9	BZ	Coumarins
83	28.67	+Na	Tetradecanol acetate	$C_{16}H_{32}O_2$	256.240 23	279.231	5.7	199.166 4	BZ	Others
84	29	+H	Phellopterin/cnidilin	$C_{17}H_{16}O_5$	300.099 77	301.106 5	−1.7	233.043 9, 218.022 6, 134.035 5	BZ	Coumarins
85	29.01	+H	5-Hydroxy-8-methoxypsoralen	$C_{12}H_8O_5$	232.037 17	233.043 4	−4.4	218.022 6	BZ	Coumarins
86	29.42	+H	Osthole	$C_{15}H_{16}O_3$	244.109 94	245.115 9	−5.2	104.104 7	BZ	Coumarins
87	29.7	+K	1-Dodecanol	$C_{12}H_{26}O$	186.198 37	225.162 3	3.3	128.060 1, 115.052 3	BZ	Essential oils
88	29.7	+K	2-Methyl-2-hexanol	$C_7H_{16}O$	116.120 12	155.084 4	7.3	86.096 6	BZ	Others
89	29.7	+Na	*α*-Santalol	$C_{15}H_{24}O$	220.182 72	243.173 2	5	184.074 0, 153.066 5	BZ	Terpenoids
90	29.78	+Na	*β*-Sitosterol	$C_{29}H_{50}O$	414.386 17	437.372 5	−6.6	276.063 5, 124.999 5	YHS	Steroids

Continued

NO.	Observed RT/min	Adducts	Component name	Formular	Neutral mass (*m*/*z*)	Observed *m*/*z*	Mass error (ppm)	Fragments	Source	Category
91	29.82	+Na	Palmitic acid	$C_{16}H_{32}O_2$	256.240 23	279.231 3	6.8	199.171 4, 184.074 0, 86.096 6	YHS	Organic acids
92	30.1	+H	Dihydrochelerythrine	$C_{21}H_{19}NO_4$	349.131 41	350.137 7	−2.8	334.110 8	YHS	Isoquinolines
93	30.11	+H	5-(2-Propenyl)-1,3-benzodioxole/*trans*-isosafrole	$C_{10}H_{10}O_2$	162.068 08	163.074 4	−5.6	67.051 8, 86.096 6	BZ	Coumarins
94	30.34	+K	*N*,*N*-dimethyl-*N*',*N*',-dimethyl-diphenyl-one	$C_{17}H_{20}N_2O$	268.157 56	307.118 1	−8.4	149.021 7, 121.029 2	YHS	Others
95	30.34	+Na	Diisobutyl phthalate	$C_{16}H_{22}O_4$	278.151 81	301.14	−3.3	149.021 7	BZ	Others
96	30.35	+Na	5-Hydroxymethylfurfural	$C_6H_6O_3$	126.031 69	149.022	7	86.096 6	BZ	Aldehydes
97	30.65	+H	Anhydrobyankangelicin/apaensin/byakangelicol	$C_{17}H_{16}O_6$	316.094 69	317.101 8	−0.6	233.043 9, 218.022 6, 203.034 9, 175.037 5	BZ	Coumarins
98	31	+H	Nerolidol	$C_{15}H_{26}O$	222.198 37	223.204 5	−4.9	207.031 8, 171.138 3	BZ	Terpenoids
99	31.19	+Na	1-Tetradecanol	$C_{14}H_{30}O$	214.229 67	237.220 2	5.6	199.166 4, 184.074 0, 171.138 3, 89.057 9	BZ	Essential oils
100	31.35	+Na	1-Hexadecanol	$C_{16}H_{34}O$	242.260 97	265.251 8	6	199.166 4, 171.138 3	BZ	Essential oils

2 动物实验验证

2.1 对扭体次数和扭体潜伏期的影响 PD的主要行为学特征之一是前列腺素等介质异常引起的子宫平滑肌过度收缩, 从而导致实验动物出现明显的扭体反应, 其扭体次数反映疼痛反应的严重程度, 而扭体潜伏期则代表疼痛发生的迟缓程度, 二者是评价镇痛作用的重要指标。与model组比较, YZOL各剂量组及ibuprofen组大鼠扭体次数显著减少 ($P < 0.05$), YZOL各剂量组及ibuprofen组大鼠扭体潜伏期明显延长 ($P < 0.05$), 提示YZOL能够有效减轻疼痛反应、延缓疼痛发生, 具有显著的镇痛作用 (表2)。

Table 2 Effects of YZOL on writhing latency and writhing count in rats. YZOL-L: 1.08 g·kg^{-1}; YZOL-M: 3.24 g·kg^{-1}; YZOL-H: 9.72 g·kg^{-1}. $n = 8$, $\bar{x} \pm s$. $^{\#\#}P < 0.01$, $^{\#\#\#\#}P < 0.000\ 1$ *vs* control; $^{*}P < 0.05$, $^{***}P < 0.001$, $^{****}P < 0.000\ 1$ *vs* model

Group	Writhing latency / min	Writhing count / 30 min
Control	0	0
Model	4.88±3.23$^{\#\#}$	22.00±6.23$^{\#\#\#\#}$
Ibuprofen	10.71±2.04*	12.13±2.47****
YZOL-L	10.25±0.39*	16.75±2.25*
YZOL-M	10.74±1.39*	16.38±2.50*
YZOL-H	11.49±7.52*	12.67±2.16***

2.2 对大鼠痛经疼痛相关因子表达的影响 痛经的发生与前列腺素及血栓素/前列环素平衡失调密切相关, 其中$PGF_{2\alpha}$、PGE_2及其比值升高可增强子宫平滑肌收缩, 导致缺血缺氧与疼痛[27]; 而TXB_2、6-keto-$PGF_{1\alpha}$及其比值失衡则促进血管收缩和血小板聚集, 加剧子宫血流障碍, 进一步诱发或加剧痛经症状[28]。与control相比, model组大鼠子宫匀浆液中$PGF_{2\alpha}$水平显著升高 ($P < 0.000\ 1$)、PGE_2水平显著降低 ($P < 0.05$)、$PGF_{2\alpha}/PGE_2$显著升高 ($P < 0.000\ 1$); TXB_2水平无显著差异, 6-keto-$PGF_{1\alpha}$水平显著下降 ($P < 0.01$), TXB_2/6-keto-$PGF_{1\alpha}$显著升高 ($P < 0.000\ 1$)。与model相比, YZOL-M, YZOL-H及ibuprofen组$PGF_{2\alpha}$水平显著下降 ($P < 0.01$); YZOL各剂量组及ibuprofen组间PGE_2水平无显著性差异; YZOL-M、YZOL-H及ibuprofen $PGF_{2\alpha}/PGE_2$水平显著降低 ($P < 0.05$)。YZOL各剂量组及ibuprofen TXB_2水平无显著性差异; YZOL-H及ibuprofen 6-keto-$PGF_{1\alpha}$水平显著升高 ($P < 0.05$); YZOL-L、YZOL-M、YZOL-H及ibuprofen TXB_2/6-keto-$PGF_{1\alpha}$显著降低 ($P < 0.05$) (图2)。

2.3 大鼠子宫组织和卵巢病理学形态分析 H&E染色结果显示, control组大鼠子宫组织结构清晰, 由内向外分别为子宫内膜、子宫肌层和子宫外膜, 排列整齐紧密, 子宫内膜上皮细胞完整, 子宫内膜及肌层厚度正常, 宫腔通畅; model组子宫壁变薄, 子宫结构紊乱, 宫腔不光滑, 子宫内膜增生明显, 肌层增生明显; 与model比较, YZOL-L、YZOL-M、YZOL-H的宫腔趋于光滑, 肌层增生减轻, 其中YZOL-H子宫状态最趋近于正常对照组。Control组卵泡结构清晰排列整齐, model闭锁卵泡数增多, 卵泡排列紊乱, 黄体半径增大; 与model较, YZOL-L、YZOL-M、YZOL-H闭锁卵泡数减少, 卵泡排列相对整齐 (图3)。

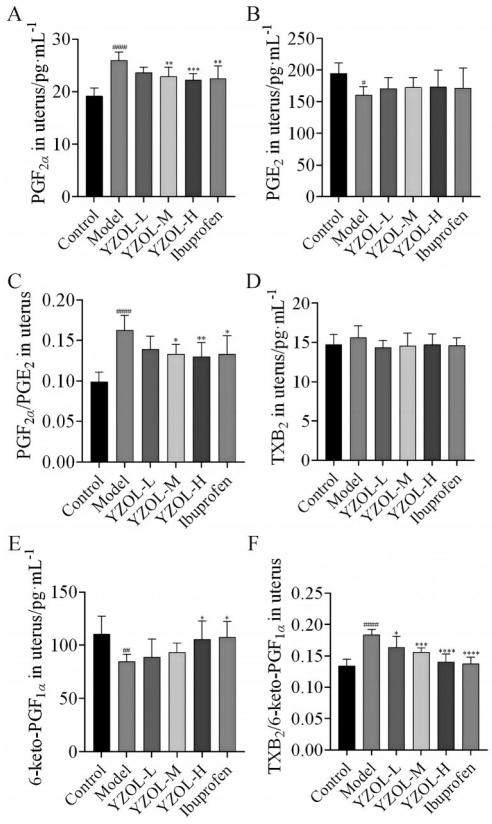


Figure 2　The levels of $PGF_{2\alpha}$, PGE_2 and $PGF_{2\alpha}/PGE_2$, TXB_2, 6-keto-$PGF_{1\alpha}$ and TXB_2/6-keto-$PGF_{1\alpha}$ in uterine tissue of rats in all groups were compared. $n = 8$, $\bar{x} \pm s$. $^{\#}P < 0.05$, $^{\#\#}P < 0.01$, $^{\#\#\#}P < 0.001$, $^{\#\#\#\#}P < 0.000\ 1$ *vs* control; $^{*}P < 0.05$, $^{**}P < 0.01$, $^{***}P < 0.001$, $^{****}P < 0.000\ 1$ *vs* model. $PGF_{2\alpha}$: Prostaglandin $F_{2\alpha}$; PGE_2: Prostaglandin E2; TXB_2: Thromboxane B2; 6-keto-$PGF_{1\alpha}$: 6-Keto-prostaglandin $F_{1\alpha}$

3　转录组学研究

3.1　筛选差异表达基因　对 control (Con)、model (Mod) 和 YZOL-H 组表达的基因进行分析, Mod *vs* Con 得到 4 916 个 DEGs, 其中, 上调数目为 1 214 个, 下调数目为 3 702 个; YZOL-H *vs* Mod 得到 1 777 个 DEGs, 其中, 上调数目为 854 个, 下调数目为 932 个。将筛选出的 DEGs 进行聚类分析, 显示各组之间分布差异明显, 结果显示组间差异显著, 组内 DEGs 表达具有较高一致性。进一步分析发现, YZOL 共回调了 403 个基因, 其中造模后有 123 个基因上调, 给药治疗后下调; 造模后 280 个基因下调, 给药治疗后上调。

3.2　差异表达基因的功能富集分析　通过对 403 个回调基因进行 GO 富集分析, 共获得 1 343 个条目, 其中 BP (biological process) 相关条目 331 个, 主要集中在细胞周期过程、有丝分裂相关过程、DNA 复制起始、蛋白质磷酸化调控以及细胞外刺激应答等方面; CC (cellular component) 653 个, 主要涉及质膜、突触后膜、谷氨酸

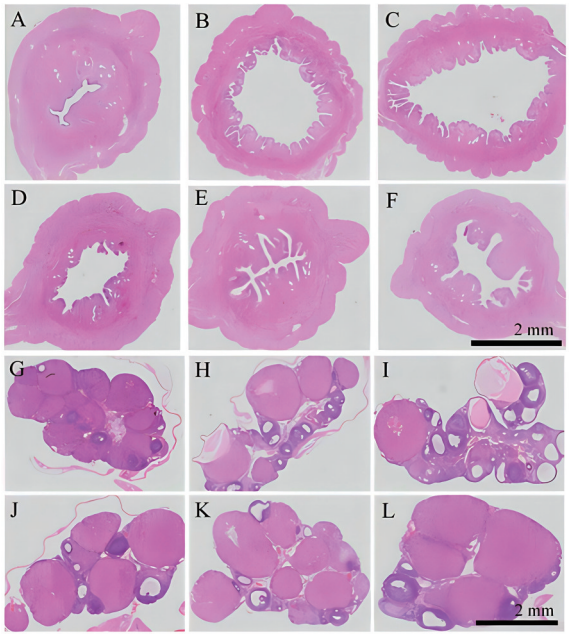


Figure 3　Representative H&E staining of rat uterine (A－F) and ovarian (G－L) tissues (×20) from the control, model, YZOL-L, YZOL-M, YZOL-H, and ibuprofen groups

受体复合体、外包膜结构以及胞质细胞骨架相关复合体等; MF (molecular function) 359 个, 主要包括信号受体结合、转运体活性、离子通道活性、神经递质受体活性、蛋白质激酶结合及 G 蛋白偶联受体活性等。细胞周期和 DNA 复制与子宫内膜的周期性变化相关[29], 蛋白质磷酸化及细胞外刺激应答参与前列腺素和炎症信号的调控[30]; 质膜及突触后膜受体复合体介导疼痛信号传递[31], 而离子通道和 GPCR 活性在子宫平滑肌收缩及痛觉信号放大过程中发挥重要调节作用[32]。同时, 通过对差异基因进行 KEGG 富集分析, 共获得 272 条通路, 主要富集于神经活性配体–受体相互作用、TGF-β 信号通路、Rap1 信号通路、PI3K-Akt 信号通路、卵巢类固醇生成、TRP 通道炎症介质调控、MAPK 信号通路等。神经活性配体–受体相互作用、TRP 通道炎症介质调控等涉及疼痛信号的传递与敏化[33,34]; TGF-β、MAPK、PI3K-Akt 等信号通路参与炎症反应及子宫平滑肌收缩调控[35-37]; 卵巢类固醇生成则与性激素水平异常及内膜周期性改变有关[38]。

4　YZOL 干预 PD 的网络调控作用分析

基于转录组测序所识别的 YZOL 关键调控基因及其作用通路, 构建了 YZOL 治疗 PD 的“活性成分–关键靶点–信号通路–病理环节–药效作用”整合网络 (图 4)。结果显示, YZOL 主要通过黄连碱、紫花前胡苷、补骨脂素醇、二氢白屈菜红碱、欧前胡素等代表性活性成分, 共同调控以下多条信号通路以发挥综合治疗作用:

调控疼痛感知与传导异常, 涉及神经活性配体−受体相互作用、谷氨酸能突触等神经递质相关通路; 干预子宫平滑肌收缩及缺血缺氧过程, 涉及PI3K-Akt、MAPK及HIF-1信号通路; 调节前列腺素及其他炎症介质的合成与释放, 涉及NF-κB和TRP通道等炎症相关通路; 恢复激素与钙离子信号平衡, 涉及卵巢类固醇生成和PPAR信号通路, 从而促进性激素与钙离子稳态的恢复。此外, 部分基因参与免疫与炎症反应失衡过程(如细胞因子−受体相互作用及TGF-β信号通路), 提示YZOL可能通过调节免疫炎症反应及细胞死亡平衡来改善局部炎症微环境。综上所述, YZOL可能通过协同调控痛觉信号传导、缓解子宫痉挛与改善血流灌注、平衡前列腺素水平、恢复激素信号稳态以及重建免疫−炎症稳态等多条通路, 形成系统性治疗网络, 从而发挥对PD的综合治疗作用。

5 分子对接验证关键成分与靶点的相互作用

采用AutoDock Vina对YZOL主要活性成分与7个关键靶点进行分子对接分析。结果(表3)显示, 大部分成分与靶点的结合能较低, 说明其具有较强的结合稳定性。延胡索来源的白屈菜红碱、黄连碱、二氢白屈菜红碱及白芷来源的欧前胡素、紫花前胡苷等与多个靶点结合紧密, 其结合能力与阳性化合物相当或更强。此外, 参考公开数据库(TCMSP、ETCM等)报道的ADME参数, 这些成分具有一定的口服生物利用度(OB)和药代动力学特征, 其中大部分成分的OB值达到或超过30%, 提示其在体内可能具备较好的吸收与利用潜力。综合结合能与OB值结果可见, YZOL中的多种成分兼具较强的受体亲和力和潜在的体内可利用性。结合模式分析进一步显示, 活性成分可通过氢键等非共价相互作用稳定结合于靶点活性位点(图5), 从分子水平支持了其多成分、多靶点协同镇痛的作用机制。

讨论

PD的高发病率和周期性反复发作, 严重影响女性身心健康, 对家庭及社会发展亦具有不良影响, 已成为公共卫生关注问题。本研究结果表明, YZOL中的化学成分以生物碱类、香豆素类化合物为主。其中, YZOL中的延胡索乙素、盐酸巴马汀、原阿片碱等是发挥镇痛作用的主要成分[39]。PD的核心病理机制在于子宫平滑肌的痉挛性收缩与缺血缺氧, 本研究通过皮下注射苯甲酸雌二醇和腹腔注射缩宫素的方法复制大鼠PD模型, 连续注射苯甲酸雌二醇可提高大鼠子宫敏感性, 最后一天注射缩宫素会导致大鼠子宫平滑肌收缩, 同时提高子宫内膜合成与释放$PGF_{2\alpha}$, 两者共同作用, 为目前广泛应用的PD大鼠建模方法。本实验中模型组大鼠与对照组相比扭体反应次数增加, 扭体潜伏期缩短, 表明PD模型构建具有良好的稳定性与可重复性。实验结果显示, YZOL不仅显著减少了扭体次数、延长了潜伏期, 更在组织病理学层面显著修复了子宫内膜损伤, 减少了闭锁卵泡数量。提示YZOL对PD大

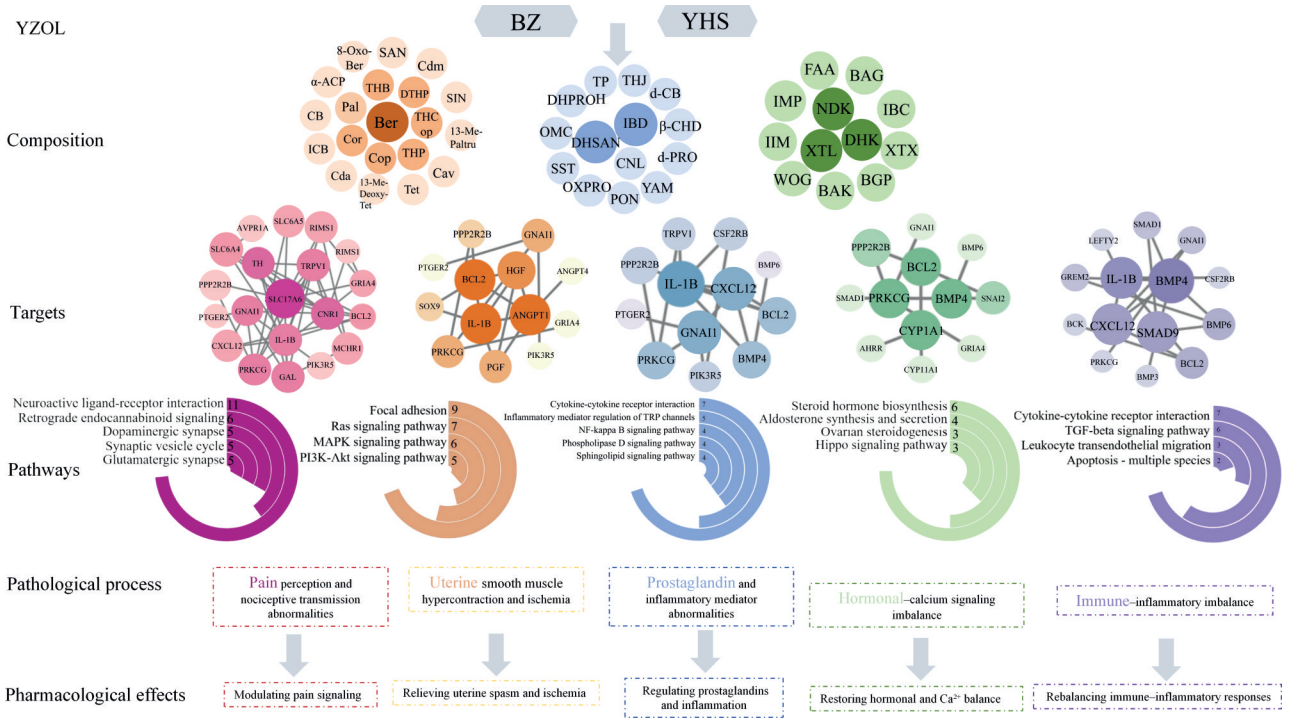


Figure 4 Integrated "component-target-pathway-pathology-effect" network of YZOL in primary dysmenorrhea

Table 3　Molecular docking results. * refers to the components identified and detailed in Table 1. OB: Oral bioavailability

Target	Positive control	Docking energy	Components of YZOL*	Docking energy	Source	OB/%
AVPR1A	Relcovaptan	−7.6	Marmesin (NO.25)	−9.1	BZ	50.28
			Bicuculline (NO.21)	−8.9	YHS	69.67
			Coptisine (NO.38)	−8.6	YHS	30.67
			Xanthotoxol (NO.66)	−8.6	BZ	29.21
			Dihydrochelerythrine (NO.92)	−8.5	YHS	32.73
CXCL12	AMD3100	−10.3	Bicuculline (NO.21)	−9.7	YHS	69.67
			Coptisine (NO.38)	−9.7	YHS	30.67
			Dihydrochelerythrine (NO.92)	−9.7	YHS	32.73
			Nodakenin (NO.26)	−9.3	BZ	57.12
CYP11A1	Aminoglutethimide	−7	Coptisine (NO.38)	−9.7	YHS	30.67
			Nodakenin (NO.26)	−9.6	BZ	57.12
IL1B	Pralnacasan	−8.2	Bicuculline (NO.21)	−8.1	YHS	69.67
			Coptisine (NO.38)	−7.5	YHS	30.67
			Isoboldine (NO.49)	−7.5	YHS	39.53
PRKCG	Staurosporine	−7.3	Coptisine (NO.38)	−6.8	YHS	30.67
			Bicuculline (NO.21)	−6.6	YHS	69.67
TRPV1	Capsaicin	−6.2	Bicuculline (NO.21)	−7.7	YHS	69.67
			Coptisine (NO.38)	−7.6	YHS	30.67
			Nodakenin (NO.26)	−7.3	BZ	57.12
PTGER2	Misoprostol	−10.19	Marmesin (NO.25)	−8.5	BZ	50.28
			Coptisine (NO.38)	−8.1	YHS	30.67
			Bicuculline (NO.21)	−7.9	YHS	69.67
			Dihydrochelerythrine (NO.92)	−7.5	YHS	32.73
			Nodakenin (NO.26)	−7.5	BZ	57.12

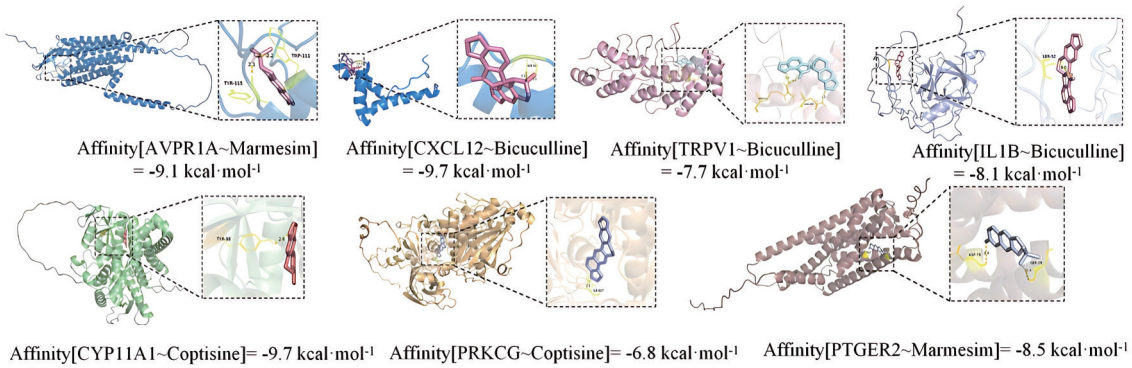


Figure 5　Molecular docking models of the chemical constituents of YZOL with core targets

鼠疼痛具有一定缓解作用, 且涉及对子宫及卵巢组织形态的一定程度的修复与保护。过多的前列腺素可能会在子宫内膜脱落时引起PD, 从而产生相对的子宫肌层过度收缩、缺血和缺氧性子宫状态。$PGF_{2\alpha}$/PGE_2比值已被广泛用于PD的临床诊断与研究指标。本实验中模型组大鼠与对照组相比, $PGF_{2\alpha}$/PGE_2显著升高, 给药后回调。此外, TXA_2有收缩血管和聚集血小板作用, 而前列腺环素 (PGI_2) 有扩张血管和抑制血小板聚集的作用, 是一对作用相反的拮抗物质。正常生理状态下TXA_2/PGI_2处于动态平衡状态, 血管内环境保持稳定。病理情况下, 两者失衡, TXA_2/PGI_2比值升高, 子宫血管平滑肌收缩, 血小板聚集, 使血液处于高凝状态, 是痛经的主要原因之一[40]。由于TXA_2和PGI_2的半衰期极短, 可迅速转变为较稳定的代谢产物TXB_2和6-keto-$PGF_{1\alpha}$, 血浆中两者的浓度可反映体内TXA_2和PGI_2的水平[41]。本实验中模型组大鼠与对照组相比, TXB_2/6-keto-$PGF_{1\alpha}$显著升高, 给药后回调。提示YZOL可能通过扩张血管、抑制血小板聚集改善痛经, 这与转录组学筛选出的平滑肌收缩相关通路形成了相互印证。

本研究基于转录组学测序结果, 提示YZOL治疗PD可能广泛涉及TGF-β、Rap1、PI3K-Akt及神经活性配体−受体相互作用等关键通路, 从分子层面阐释了其“标本兼治”的科学内涵。在组织修复与抗炎方面, 转录组数据显示YZOL对TGF-β和MAPK信号通路相关基因表达具有回调趋势, 这与H&E染色观察到的子

宫内膜病理改善相呼应; 推测YZOL可能通过干预MAPK级联反应影响下游炎症介质释放, 并潜在借助TGF-β通路参与受损内膜的修复过程。此外, 本研究关注到Rap1与PI3K-Akt通路在细胞骨架及平滑肌调节中的潜在作用, 结合生化指标中TXB_2/6-keto-$PGF_{1\alpha}$比值的改善, 提示YZOL或许能通过PI3K-Akt/eNOS轴改善缺氧微环境, 并经由Rap1通路调节平滑肌收缩状态, 从而有助于缓解痉挛并改善局部供血。在痛觉传导方面, KEGG富集分析指向“神经活性配体−受体相互作用”通路, 结合预测到的TRPV1及PRKCG等靶点, 暗示YZOL可能通过调节外周伤害性感受器的敏感性, 干扰痛觉信号传导, 这可能是其延长PD大鼠扭体潜伏期的生物学基础之一。

为进一步探究上述药效机制的物质基础, 本研究基于UPLC-Q-TOF-MS/MS鉴定的化学成分, 对筛选出的核心靶点进行了分子对接验证, 结果初步揭示了YZOL“多成分−多靶点”的协同作用模式。通过分子对接筛选得到了YZOL治疗PD的潜在活性成分, 包括黄连碱、紫花前胡苷、补骨脂素醇、二氢白屈菜红碱、欧前胡素等。分子对接结果显示, 这些成分与疼痛及炎症等相关靶点之间结合活性良好, 提示YZOL中的活性成分可能通过调控疼痛敏化及子宫平滑肌收缩途径发挥作用。据相关文献报道, 黄连碱与紫花前胡苷均可抑制NF-κB通路活化及IL-1β、IL-6、TNF-α等炎症介质表达, 从而减轻局部炎症反应; 其中黄连碱还通过MAPK、PI3K-Akt等信号下调PGE_2生成, 可能作用于PTGER2受体轴[42,43]。补骨脂素醇在多种炎症性疼痛模型中表现出显著的镇痛作用, 可通过抑制TRPV1通道的致敏与表达、降低Ca^{2+}内流及下调炎症因子的生成发挥抗炎镇痛效应[44]。二氢白屈菜红碱属于苯并菲啶类生物碱, 其同系物白屈菜红碱为经典PKC抑制剂, 能够减弱痛觉神经元异常兴奋, 提示其可能通过PRKCG-Ca^{2+}信号通路参与镇痛[45]。欧前胡素可抑制VEGF-A诱导的VEGFR-2、Akt和ERK磷酸化, 从而抑制内皮细胞的增殖、迁移及管腔形成。该作用涉及VEGF-Akt/ERK信号通路, 与痛经研究中所报道的PI3K-Akt-HIF-1信号在调控血管反应和缺氧应答方面具有一致性[46]。综上, YZOL中的生物碱类与香豆素类活性成分可能通过调控TRPV1-Ca^{2+}信号轴、NF-κB介导的炎症通路及PKC-MAPK信号级联, 抑制炎症因子释放、减轻痛觉敏化并改善平滑肌收缩, 从而共同发挥缓解PD的多成分协同镇痛作用。

综上所述, YZOL各组分相互协同发挥整体调控作用, 可显著改善苯甲酸雌二醇与缩宫素诱导的PD模型表型。本实验对YZOL化学成分及其作用靶点进行预测分析, 并利用分子对接初步验证了YZOL干预PD的关键化学成分和关键靶点, 该研究思路与中药现代化研究中提出的整合药理学路径相一致[47-49], 进一步阐明了YZOL在PD治疗中多组分、多靶点、多途径的协同作用机制, 并为中医药防治PD的研究提供了实验依据。相关研究从不同层面揭示了YZOL镇痛机制的可能生物学基础。在疼痛传导方面, TRPV1被认为是重要的感觉通道蛋白, 其在子宫及异位内膜组织中高表达, 与疼痛敏化程度呈正相关[50]。进一步的研究显示, 雌激素可显著上调TRPV1在子宫内膜中的表达, 并增强其对刺激的敏感性, 表明TRPV1的表达受激素水平调控并呈周期依赖性[51]。与药物成分相关的研究显示: 延胡索生物碱l-THP在腺肌病模型中可降低子宫收缩幅度并缓解痛觉[52], 吴茱萸生物碱evodiamine能抑制Ca^{2+}激活氯通道TMEM16A, 从而降低平滑肌去极化与Ca^{2+}内流[53], 口服给药后l-THP及相关生物碱在体内可检测到稳定暴露, 提示具有良好可达性与药代学基础[54,55]。本研究的局限性主要未对关键靶点进行蛋白及mRNA水平验证, 尚未通过离体子宫条张力或细胞模型验证药物对子宫收缩及炎症反应的直接调控作用。未来研究可进一步结合qPCR、Western blot、免疫荧光等实验验证关键通路, 并通过多组学整合明确主要作用成分及其调控网络, 以期系统阐明YZOL的药效物质基础与作用网络。

作者贡献: 王萍、吴丹负责课题总体设计及文章修改等; 关建丽参与实验设计且给予实验样本支持; 许海玉给予研究思路和学术指导; 郑韩、付璐负责实验操作、数据处理及论文撰写; 钟余特、李玮婕负责实验技术指导。

利益冲突: 所有作者均声明不存在利益冲突。

References

[1] Kho KA, Shields JK. Diagnosis and management of primary dysmenorrhea [J]. JAMA, 2020, 323: 268-269.

[2] Li XL, Hao XY, Liu JH, et al. Efficacy of non-pharmacological interventions for primary dysmenorrhea: A systematic review and bayesian network meta-analysis [J]. BMJ Evid Based Med, 2024, 29: 162-170.

[3] Frank T, Kevin H. Primary dysmenorrhea: Diagnosis and therapy [J]. Obstet Gynecol, 2021, 137: 752.

[4] Osayande AS, Mehulic S. Diagnosis and initial management of dysmenorrhea [J]. Am Fam Physician, 2014, 89: 341-346.

[5] Sun T. Prevention and treatment strategies of gastrointestinal and cardiovascular adverse reactions in patients with long-term oral non-steroidal anti-inflammatory drugs [J]. Cardiovasc Dis Electron J Integr Tradit Chin West Med (中西医结合心血管病电子杂志), 2022, 10: 93-95.

[6] Chen ZY, Zhao YD, Jiang MX, et al. Overview of the etiology and pathogenesis of primary dysmenorrhea in traditional Chinese medicine [J]. Clin J Chin Med (中医临床研究), 2021, 13: 109-112.

[7] Xu M, Chen Q. Progress in clinical research on oral Chinese medicine for the treatment of primary dysmenorrhea [J]. China Naturop (中国民间疗法), 2024, 32: 107-110.

[8] Cao DM, Du GH, Zhang W. Compound Yimucao Oral Liquid in the treatment of 100 cases of menorrhagia with blood stasis type [J]. China Pharm (中国药业), 2016, 25: 92-94.

[9] Ma YR, Hu YF. Efficacy of Xuefu Zhuyu Oral Liquid on primary dysmenorrhea and its influence on coagulation status [J]. Thromb Hemost (血栓与止血学), 2022, 28: 842-843.

[10] Lei FY, Xu HP. Compound Tongjing Oral Liquid in the treatment of 60 cases of primary dysmenorrhea [J]. Forum Tradit Chin Med (国医论坛), 2007, 22: 36-37.

[11] Hu RQ, Zhao GJ. Research progress and development prospects of traditional Chinese medicine oral liquid [J]. J Baotou Med Coll (包头医学院学报), 2013, 29: 142-144.

[12] Yuan HF, He SF, Yang J, et al. Overview, strategy and prospect of stability research of traditional Chinese medicine oral liquid preparations [J]. Drug Eval (药品评价), 2023, 20: 261-264.

[13] Zhang XK, Zhang S, Yang Q, et al. Simultaneous quantitative determination of 12 active components in Yuanhu Zhitong prescription by RP-HPLC coupled with photodiode array detection [J]. Pharmacogn Mag, 2015, 11: 61-68.

[14] Liao ZG, Liang XL, Zhu JY, et al. Correlation between synergistic action of Radix *Angelica dahurica* extracts on analgesic effects of *Corydalis* alkaloid and plasma concentration of *DL*-THP [J]. J Ethnopharmacol, 2010, 129: 115-120.

[15] Zhang XH, Wang YL, Zhang K, et al. Discovery of tetrahydropalmatine and protopine regulate the expression of dopamine receptor D2 to alleviate migraine from Yuanhu Zhitong formula [J]. Phytomedicine, 2021, 91: 153702.

[16] Zhang K, Su J, Huang YT, et al. Untargeted metabolomics reveals the synergistic mechanisms of Yuanhu Zhitong Oral Liquid in the treatment of primary dysmenorrhea [J]. J Chromatogr B Analyt Technol Biomed Life Sci, 2021, 1165: 122523.

[17] Gu YB, Huang J, Guo HG, et al. A randomized controlled study for Yuanhu Zhitong dropping pills in the treatment of knee osteoarthritis [J]. Medicine (Baltimore), 2020, 99: e20666.

[18] Chinese Pharmacopoeia Commission. Pharmacopoeia of the People's Republic of China: Part I (中华人民共和国药典: 一部) [M]. Beijing: China Medical Science and Technology Press, 2025.

[19] Zhang XS. Clinical observation on Yuanhu Zhitong tablet combined with exercise in the treatment of primary dysmenorrhea of female college students [J]. Hebei J Tradit Chin Med (河北中医), 2015, 37: 904-905.

[20] Fang YS, He ZP, Zhang H, et al. Effects of medicated serum of Yuanhu Zhitong capsule on dysmenorrhea model animals [J]. Chin J Comp Med (中国比较医学杂志), 2010, 20: 35-37.

[21] Feng Y, Zhang ZP, Shen XP, et al. The study of analgesic effect and mechanism of Yuanhu Zhitong Dropping Pills on dysmenorrhea model rats [J]. China Med Her (中国医药导报), 2018, 15: 8-12.

[22] Zhang K, Li NN, Li S, et al. Study on analgesic effect and mechanism of Yuanhu Zhitong Oral Liquid on primary dysmenorrhea [J]. Tianjin J Tradit Chin Med (天津中医药), 2019, 36: 1006-1011.

[23] Fu L, Chen CY, Gao J, et al. Improvement of quality standard of Yuanhu Zhitong Oral Liquid [J]. Chin J Exp Tradit Med Formulae (中国实验方剂学杂志), 2024, 30: 125-131.

[24] Tao Y, Xu HY, Wang SS, et al. Identification of the absorbed constituents after oral administration of Yuanhu Zhitong prescription extract and its pharmacokinetic study by rapid resolution liquid chromatography/quadrupole time-of-flight [J]. J Chromatogr B, 2013, 935: 1-9.

[25] Wang P, Li K, Tao Y, et al. TCM-ADMEpred: A novel strategy for poly-pharmacokinetics prediction of traditional Chinese medicine based on single constituent pharmacokinetics, structural similarity, and mathematical modeling [J]. J Ethnopharmacol, 2019, 236: 277-287.

[26] Traditional Chinese Medicine Experimental Pharmacology Professional Committee, China Association of Chinese Medicine. Specifications for preparation of dysmenorrhea animal models (draft) [J]. Chin J Exp Tradit Med Formulae (中国实验方剂学杂志), 2018, 24: 20-24.

[27] Harel Z. Dysmenorrhea in adolescents and young adults: Etiology and management [J]. J Pediatr Adolesc Gynecol, 2006, 19: 363-371.

[28] Yang L, Cao Z, Yu B, et al. An *in vivo* mouse model of primary dysmenorrhea [J]. Exp Anim, 2015, 64: 295-303.

[29] Talbi S, Hamilton AE, Vo KC, et al. Molecular phenotyping of human endometrium distinguishes menstrual cycle phases and underlying biological processes in normo-ovulatory women [J]. Endocrinology, 2006, 147: 1097-1121.

[30] Achache H, Tsafrir A, Prus D, et al. Defective endometrial prostaglandin synthesis identified in patients with repeated implantation failure undergoing *in vitro* fertilization [J]. Fertil Steril, 2010, 94: 1935-1940.

[31] Di Maio G, Squillace A, Vellucci R, et al. Mechanisms of transmission and processing of pain: A narrative review [J]. Int J Environ Res Public Health, 2023, 20: 3064.

[32] Pehlivanoğlu B, Bayrak S, Doğan M. A close look at the contraction and relaxation of the myometrium; the role of calcium [J]. J Turk Ger Gynecol Assoc, 2013, 14: 230-234.

[33] Wangzhou A, McIlvried LA, Paige C, et al. A ligand-receptor interactome platform for discovery of pain mechanisms and therapeutic targets [J]. Cell Rep, 2021, 36: 109482.

[34] Luo J, Bavencoffe A, Yang P, et al. Targeting pain-evoking

transient receptor potential channels for the treatment of pain [J]. Neurotherapeutics, 2014, 11: 606-620.

[35] Li Q. Transforming growth factor *β* signaling in uterine development and function [J]. Reprod Biol Endocrinol, 2014, 12: 50.

[36] Wang R, Zhang Y, Wang LL, et al. Research progress of combined traditional Chinese and Western medicine in the treatment of primary dysmenorrhea based on MAPK/ERK/NF-*κ*B signaling pathway [J]. J Pract Tradit Chin Intern Med (实用中医内科杂志), 2024, 38: 90-93.

[37] Zhou Q, Xu H, Chen L, et al. Mechanism of action of Taohong Siwu decoction in the alleviation of primary dysmenorrhea [J]. Front Med (Lausanne), 2024, 11: 1343179.

[38] Szóstek AZ, Galvão AM, Ferreira-Dias GM, et al. Ovarian steroids affect prostaglandin production in equine endometrial cells *in vitro* [J]. J Endocrinol, 2014, 220: 263-276.

[39] Li YF, Zhao MF, Tang R, et al. Research on the material basis of analgesic effect of processed Rhizoma Corydalis from Zhejiang province based on chemometrics [J]. Chin J Mod Appl Pharm (中国现代应用药学), 2024, 41: 1892-1899.

[40] Peng ZP, Teng JX, Dang HZ, et al. Study on the effect of regulating Qi and activating blood to stop pain on hemorheology and prostaglandin changes in rats with dysmenorrhea [J]. Chin J Integr Tradit West Med Intensive Crit Care (中国中西医结合急救杂志), 2002, 9: 95-97.

[41] Zheng LM, Ji GF, Ma DD, et al. Clinical analysis of plasma thromboxane B_2 and 6-keto-prostaglandin $F_1\alpha$ in patients with cerebrovascular disease and myocardial infarction [J]. Clin Focus (临床荟萃), 1994, 9: 769-770.

[42] Rim HK, Cho W, Kim YS, et al. Nodakenin inhibits LPS-induced inflammatory cytokine production *via* suppression of NF-*κ*B activation in macrophages [J]. J Pharmacol Exp Ther, 2012, 341: 255-264.

[43] Li Z, Zhou J, Wang Q, et al. Nodakenetin alleviates CFA-induced inflammatory pain through suppression of NF-*κ*B signaling pathway [J]. Biomed Pharmacother, 2022, 156: 113971.

[44] Zhang Y, Li X, Zhao H, et al. Xanthotoxol attenuates inflammatory and neuropathic pain by inhibiting TRPV1 channel sensitization [J]. Eur J Pharmacol, 2023, 942: 175524.

[45] Li Y, Chen L, Chen J, et al. PKC inhibition attenuates heat hyperalgesia in mice *via* TRPV1 modulation [J]. Sci Rep, 2018, 8: 10341.

[46] Kim JH, Kim JK, Ahn EK, et al. Marmesin is a novel angiogenesis inhibitor: Regulatory effect and molecular mechanism on endothelial cell fate and angiogenesis [J]. Cancer Lett, 2015, 369: 323-330.

[47] Liu Q, Zhang D, Wang B, et al. Network pharmacology: Advancing the application of large language models in traditional Chinese medicine research [J]. Sci Tradit Chin Med, 2025, 3: 113-123.

[48] Li Z, Yang L, Kong L, et al. Drug innovation *via* integration of traditional Chinese and Western medicine [J]. Sci Tradit Chin Med, 2025, 3: 97-112.

[49] Wang Y, Yang Z, Wu J, et al. Development and challenges of mass spectrometry database for traditional Chinese medicine: A review [J]. Sci Tradit Chin Med, 2025, 3: 210-221.

[50] Liu J, Liu X, Duan K, et al. The expression and functionality of transient receptor potential vanilloid 1 in ovarian endometriomas [J]. Reprod Sci, 2012, 19: 1110-1124.

[51] Pohóczky K, Kun J, Szalontai B, et al. Estrogen-dependent up-regulation of TRPA1 and TRPV1 receptor proteins in the rat endometrium [J]. J Mol Endocrinol, 2016, 56: 135-149.

[52] Mao X, Wang Y, Carter AV, et al. The retardation of myometrial infiltration, reduction of uterine contractility, and alleviation of generalized hyperalgesia in mice with induced adenomyosis by levo-tetrahydropalmatine (*L*-THP) and andrographolide [J]. Reprod Sci, 2011, 18: 1025-1037.

[53] Zhao Z, Xue Y, Zhang G, et al. Identification of evodiamine and rutecarpine as novel TMEM16A inhibitors and their inhibitory effects on peristalsis in isolated guinea-pig ileum [J]. Eur J Pharmacol, 2021, 908: 174340.

[54] Hong ZY, Fan GR, Chai YF, et al. Stereoselective pharmacokinetics of tetrahydropalmatine in rats [J]. Acta Pharm Sin (药学学报), 2005, 40: 746-749.

[55] Hong Z, Fan G, Le J, et al. Brain pharmacokinetics and tissue distribution of tetrahydropalmatine enantiomers in rats after oral administration of the racemate [J]. Biopharm Drug Dispos, 2006, 27: 111-117.